

DOI: 10.1002/cmdc.201300523

# Structural Optimization and Biological Screening of a Steroidal Scaffold Possessing Cucurbitacin-Like Functionalities as B-Raf Inhibitors

Mahmoud S. Ahmed, Lucas C. Kopel, and Fathi T. Halaweish\*<sup>[a]</sup>

Inhibition of the mitogen-activated protein kinase (MAPK) pathway by targeting the commonly occurring mutated B-Raf in melanoma has become a practical method for the development of drugs and drug candidates. In order to expand upon the currently reported structural scaffolds used to target the MAPK pathway, molecular docking studies led to the installation of an  $\alpha,\beta$ -unsaturated ketone side chain, related to the cucurbitacin class of natural products, on to an estrone core via an aldol condensation reaction, along with installation of the  $\Delta^{9,11}$  olefin to assemble what has been defined as a pseudo-*cis* configuration at the B/C ring juncture. Combination of these cucurbitacin-like features resulted in a compound with an enhanced biological profile against the A-375 mutant B-Raf cell line, in regards to their cytotoxicity and inhibitory activity toward phosphorylated extracellular-signal-regulated kinase (ERK).

Natural products have been an important source for drug discovery over the years. They are commonly used directly, or indirectly via semi-synthetic modifications to their structures in order to potentiate their activity, in an attempt to solve various clinical problems. Natural products continue to show potential as sources for drug candidates targeting a wide range of applications: antihypertensive, antidiabetics, antibacterial, antifungal, antimicrobial, and anticancer agents.<sup>[1]</sup>

Cucurbitacins are highly oxygenated triterpene natural products, found mainly in the Cucurbitaceae family of plants, that possess an array of biological activities: anti-inflammatory, hepatoprotective and antiproliferative activities against various cancer cell lines.<sup>[2]</sup> However, only a limited number of studies have been reported describing the biological effect of cucurbitacins towards melanoma cell lines,<sup>[3]</sup> as well as their ability to target the mitogen-activated protein kinase (MAPK) pathway, a target for the treatment of melanoma.<sup>[4]</sup> The Ras/Raf/MEK/ERK signaling pathway is a kinase receptor pathway that has been heavily studied for the treatment of melanoma due to its major role in multiple cellular processes, such as proliferation, differentiation, survival, and apoptosis.<sup>[5]</sup> B-Raf mutations show high incidence, about 66%, in melanoma. The most common mutation (~90%) is the change of Val600 to Glu in the activa-

tion loop.<sup>[6]</sup> This mutation keeps the kinase pathway constitutively active, leading to aberrant growth of melanoma cells. Therefore, inhibition of the MAPK signaling cascade at the level of B-Raf provides an approach for the treatment of melanoma.

Cucurbitacins exhibit a broad spectrum of biological activities because of their ability to target multiple biological pathways, sometimes undesirably.<sup>[7]</sup> However, this does not eliminate them as a potential source for drug development. Structural modifications to natural products and their derivatives continue to allow for increased selectivity in regards to a desired biological response, while at the same time decreasing adverse effects.<sup>[8]</sup> Instrumental to this process is the identification of important structural features that will remain and which to modify or replace.

Cucurbitacin analogues resulting from synthetic transformations on the isolated natural products have already been shown by Guo et al., Lang et al., and Bartalis et al. to have significant effects on the cytotoxicity of these compounds towards various cancer cell lines.<sup>[9]</sup> The structure-activity relationships of cucurbitacins suggests the importance of the 23,24-olefin of the  $\alpha,\beta$ -unsaturated ketone side chain.<sup>[10]</sup> Therefore, the side chain containing an enone was identified as an important pharmacophore to maintain during analogue development. This leaves the tetracyclic core for further modification.

Upon first glance at the chemical structure of cucurbitacins, known as [19(10 $\rightarrow$ 9 $\beta$ )-abeo-10 $\alpha$ -lanost-5-ene],<sup>[2d]</sup> one recognizes the similarities they possess with steroids (Figure 1). However, the cucurbitane ring system differs from that of steroids by the presence of a C-19 methyl group at C-9 instead of the usual C-10 position and the relative orientation at the B/C ring juncture—*cis* for cucurbitacins and *trans* for steroids. Due to their similarities and the ability to install new functionality, a steroid core was identified as a potential replacement for the highly functionalized tetracyclic core of the cucurbitacins.<sup>[11]</sup> In particular, the estrone skeleton was identified for derivatization due to the synthetic ability to install various functionalities while affecting the geometry of the B/C ring juncture, a key structural element of the cucurbitacin scaffold. Support for this decision comes from the ability of estrogen analogues to affect other biological processes without producing the negative side effects associated with estrogen treatment.<sup>[12]</sup>

In an effort to maximize analogue development for targeting the MAPK pathway, molecular modeling was used to investigate the installation of key structural features by systematically integrating cucurbitacin functionality with the steroidal skeleton and docking these virtual compounds against the mutant

[a] M. S. Ahmed, Dr. L. C. Kopel, Prof. Dr. F. T. Halaweish  
Department of Chemistry & Biochemistry, South Dakota State University  
Box 2202, Brookings, SD 57007 (USA)  
E-mail: fathi.halaweish@sdstate.edu

Supporting information for this article is available on the WWW under  
<http://dx.doi.org/10.1002/cmdc.201300523>.

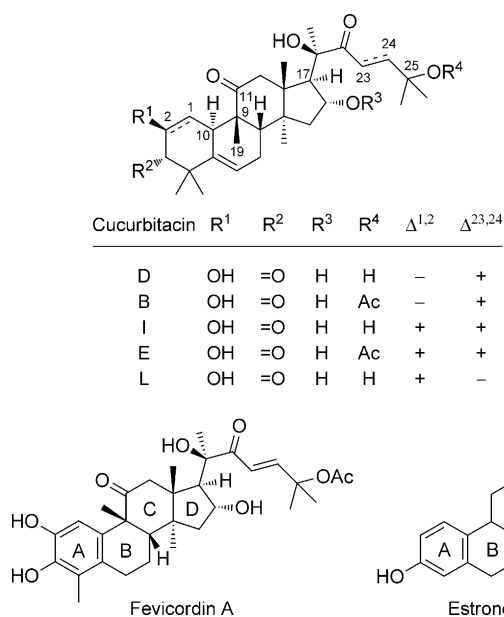


Figure 1. Structures of relevant cucurbitacins and estrone starting materials.

B-Raf receptor.<sup>[13]</sup> The two structural regions of the estrone scaffold explored were 1) incorporation of various substituted enone side chains at the C-17 position, and 2) modification of the B/C ring juncture, as shown in Figure 2.

The molecular docking studies were conducted using OpenEye Scientific Software: Fast Rigid Exhaustive Docking (FRED) Receptor, Omega,<sup>[14]</sup> FRED<sup>[15]</sup> and VIDA. The molecular docking results revealed significant binding affinity towards the crystal structure of mutant B-Raf for the estrone derivatives containing

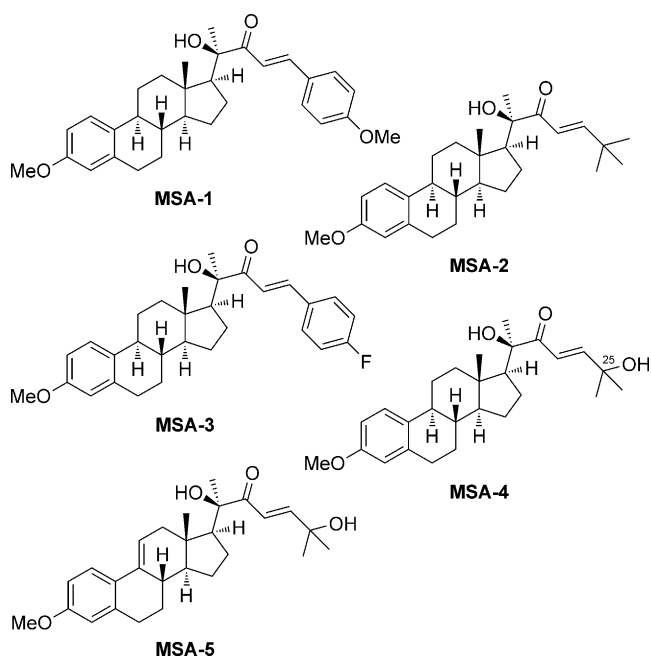


Figure 2. Modifications to the steroidal skeleton identified via molecular docking.

aliphatic- and aromatic-substituted  $\alpha,\beta$ -unsaturated ketones on the side chain, when compared with the known B-Raf inhibitor PLX-4032. The binding modes of alkyl- and aromatic-substituted enone systems installed on the estrone skeleton, such as **MSA-1**, **MSA-2** and **MSA-3**, showed hydrophobic–hydrophobic interactions. Upon installation of the cucurbitacin D side chain to the steroidal skeleton to form **MSA-4**, the binding affinity was improved via hydrophobic–hydrophobic interactions and a hydrogen-bonding interaction between the hydroxy group at C-25 and Asp 594:A in the Asp-Phe-Gly (DFG) motif. Meanwhile, installation of the  $\Delta^{9,11}$  olefin at the B/C ring juncture of **MSA-4** to obtain **MSA-5** showed a greater predicted binding affinity via the hydrogen-bonding interaction between the carbonyl of the  $\alpha,\beta$ -unsaturated ketone and Asp594:A in the DFG motif, as shown in Figure 3.

Previously reported synthetic efforts towards assembling the  $\alpha,\beta$ -unsaturated ketone side chain onto the steroidal scaffold involved taking advantage of the aldol coupling reaction, by

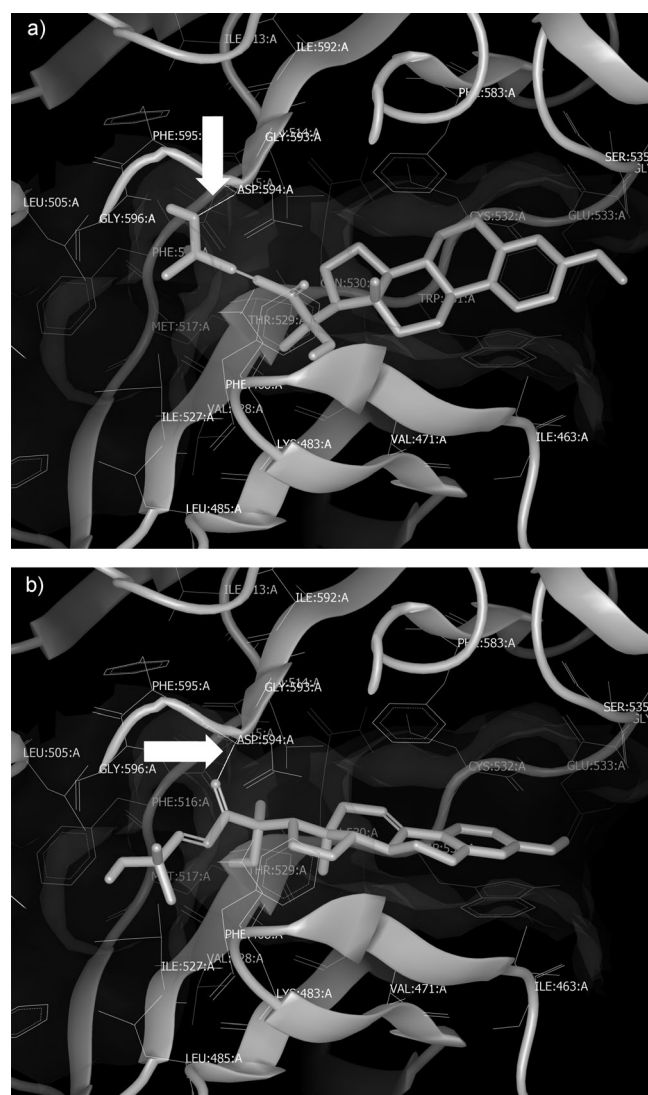
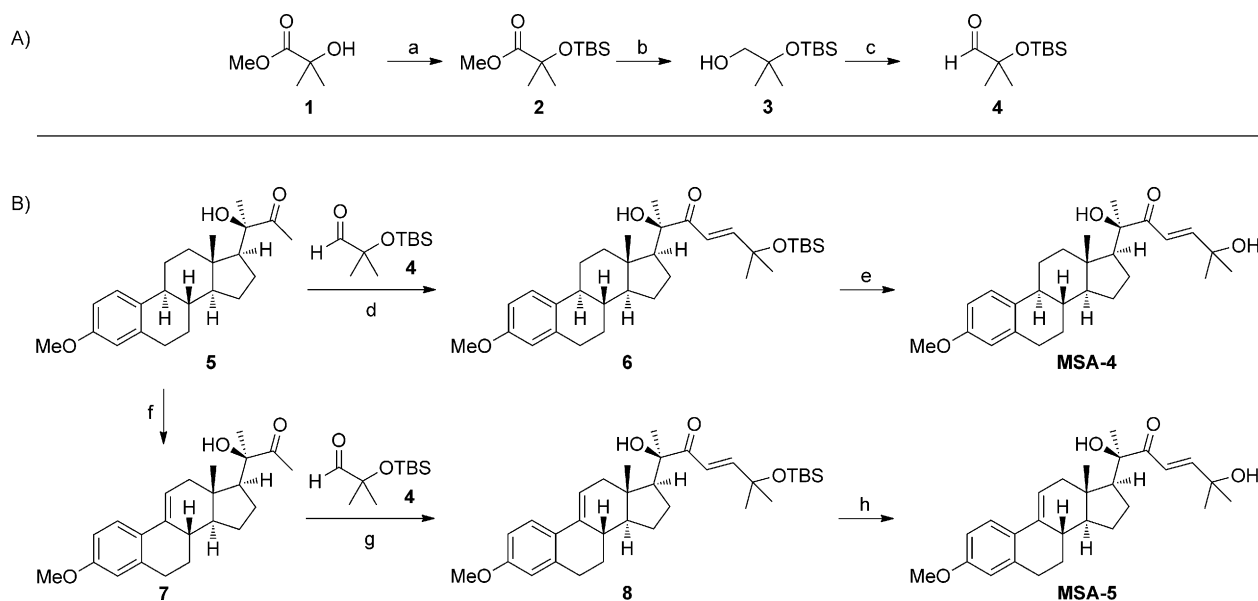


Figure 3. Visual Representation of A) **MSA-4** and B) **MSA-5** in the ATP binding site of B-Raf V<sup>600E</sup>, where the arrow shows hydrogen bond with Asp 594:A.



**Scheme 1.** A) Synthesis of reagent **4** and B) synthesis of analogue **MSA-4** and installation of a  $\Delta^{9,11}$  olefin at the B/C ring juncture for the synthesis of **MSA-5**. Reagents and conditions: a) TBSCl, imidazole, DMF, 70%; b) DIBAL-H, hexane,  $-78^\circ\text{C}$ , 80%; c) TPAP, NMO,  $\text{CH}_2\text{Cl}_2$ , 4 Å, 51%; d) LDA, THF,  $-78^\circ\text{C}$ , 58%; e) TBAF, THF, 60%; f) DDQ, MeOH,  $\text{CH}_2\text{Cl}_2$ , 80%; g) LDA, THF,  $-78^\circ\text{C}$ , 60%; h) TBAF, THF, 70%.

reacting the desired  $\alpha$ -hydroxy ketone (**5**) with various commercially available aldehydes, followed by in situ elimination to form the enone.<sup>[16]</sup> The aldol reaction here allows for the installation of a wide range of substituents onto the  $\alpha,\beta$ -unsaturated ketone, simply by changing the aldehyde fragment. The new analogue (**MSA-3**) was synthesized via the previously described method.<sup>[16]</sup> Unfortunately, the aldehyde fragment needed for installation of the cucurbitacin D side chain required synthesis.

The three-step synthetic sequence to aldehyde **4** began with protection of methyl 2-hydroxyisobutyrate (**1**) with *tert*-butyldimethylsilyl chloride (TBSCl) (Scheme 1A).<sup>[17]</sup> The resulting ester was reduced with diisobutylaluminum hydride (DIBAL-H) to afford alcohol **3** in 80% yield. This was followed by a controlled oxidation using tetrapropylammonium per-ruthenate (TPAP) and *N*-methylmorpholine *N*-oxide (NMO) to arrive at desired volatile aldehyde **4** in 51% yield.

Attempts to react  $\alpha$ -hydroxy ketone **5** with protected aldehyde **4** via an aldol condensation reaction using lithium hydroxide as the base, in a refluxing mixture of THF/water, resulted in the recovery of starting ketone **5** and the disappearance of aldehyde **4**. Therefore, an alternative procedure was used involving preforming the enolate with lithium diisopropylamine (LDA) at  $-78^\circ\text{C}$ , followed by addition of TBS-protected aldehyde **4** and warming the reaction mixture to room temperature to yield enone **6** in 58% yield, along with some unreacted ketone **5**. Final treatment of enone **6** with tetrabutylammonium fluoride (TBAF) provided **MSA-4** in 60% yield (Scheme 1B).<sup>[18]</sup>

Upon completing the installation of the cucurbitacin D side chain onto the estrone core, attention was directed toward the installation of the  $\Delta^{9,11}$  olefin at the B/C ring juncture of the steroidal skeleton to attain the pseudo-*cis* configuration. Expo-

sure of hydroxy ketone **5** to 2,3-dichloro-5,6-dicyano-1,4-benzoquinone (DDQ) in dichloromethane provided the newly formed alkene at C-9 and C-11 in 80% yield.<sup>[19]</sup> The resulting ketone was then treated with identical aldol and silyl deprotection conditions as before to afford enone **8** and **MSA-5** in 60% and 70% yields, respectively, completing this initial series of synthesized analogues (Scheme 1B).

The synthesized analogues were consequently subjected to in vitro biological screening to validate their ability to target the MAPK pathway by initially employing an MTT cell viability assay. Analogues **MSA-1**, **MSA-2** and **MSA-3** exhibited modest cytotoxicity with  $\text{IC}_{50}$  values ranging from 20–30  $\mu\text{M}$  towards the mutant B-Raf A-375 cell line, while **MSA-4** and **MSA-5** displayed improved inhibitory activity towards the same cell line. The higher  $\text{IC}_{50}$  values for **MSA-1**, **MSA-2**, and **MSA-3** can potentially be attributed to their higher  $\log P$  values.<sup>[20]</sup> Their high lipophilicity can lead to a greater plasma-protein binding affinity, which can lead to higher  $\text{IC}_{50}$  values. The lipophilicity profiles for **MSA-4** and **MSA-5** appear to be improved compared with the other analogues and are hypothesized to have a direct impact on the activity, as shown in Table 1.

Cucurbitacins were previously shown to possess inhibitory activity towards phosphorylated extracellular-signal-regulated kinase (ERK), as well as total ERK levels.<sup>[4a]</sup> This was attributed to the ability of cucurbitacins to target multiple biological targets without any specificity. However, when cucurbitacin analogues **MSA-4** and **MSA-5** were tested employing a cell-based enzyme-linked immunosorbent assay (ELISA) in A-375 melanoma cells, the synthesized analogues showed the ability to only inhibit the phosphorylated ERK levels induced by epidermal growth factor (EGF), as shown in Figure 4.

In conclusion, steroidal analogues were designed using molecular modeling in order to mimic the cucurbitacin skeleton

Compd	IC <sub>50</sub> [μM] <sup>[a]</sup>	MW [g mol <sup>-1</sup> ]	cLogP <sup>[b]</sup>
MSA-1	26.80 ± 0.44	474.63	6.30 ± 0.98
MSA-2	30.74 ± 1.90	424.61	6.23 ± 0.80
MSA-3	27.59 ± 0.12	462.59	6.51 ± 0.86
MSA-4	19.90 ± 0.21	426.78	4.86 ± 0.74
MSA-5	12.20 ± 0.12	424.57	4.58 ± 0.92
PLX-4032	3.01 ± 0.30	413.82	3.42 ± 0.49

[a] Data represent the mean ± SEM of *n* = 3 independent experiments performed in triplicate. [b] Calculated LogP values were determined using ALOGPS 2.1, and data represent the correlation between the IC<sub>50</sub>, the molecular weight, and the lipophilicity profile of the tested compounds.

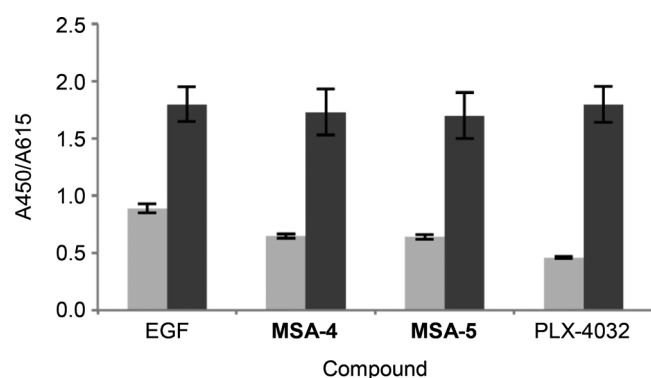


**Figure 4.** Graphical representation for the inhibitory effect of the MSA analogues over the total (■) and phosphorylated (■) ERK expression induced by epidermal growth factor (EGF).

and their ability to bind to the mutant B-Raf receptor, while attempting to increase activity and selectivity. A variety of side chains containing substituted  $\alpha,\beta$ -unsaturated ketones were assembled at the C-17 position of estrone via aldol condensation reactions using different aldehydes, such as *para*-fluorobenzaldehyde, *para*-methoxybenzaldehyde, pivaldehyde, and TBS-protected 2-hydroxy isobutyraldehyde (**4**). The cytotoxicity data exhibited the following increasing order of activity with respect to substitution on the enone: *tert*-butyl (**MSA-2**) < *para*-fluorophenyl (**MSA-3**) < *para*-methoxyphenyl (**MSA-1**) < propan-2-ol (**MSA-4**). Added modification of the estrone core of **MSA-4** by formation of the  $\Delta^{9,11}$  olefin at the B/C ring juncture provided **MSA-5** with what has been classified as a pseudo-*cis* configuration. This change in the structure led to an improvement in the activity of **MSA-5** compared with **MSA-4**, exhibiting greater cytotoxicity and inhibitory activity toward phosphorylated ERK by up to 33%.

## Experimental Section

### Molecular modeling

**2D and 3D Structures:** A virtual library of 100 structurally modified C-17 estrone analogues containing an enone side chain, standard cucurbitacins, and known mutant B-Raf inhibitors were prepared

using ChemOffice Ultra 2004 (CambridgeSoft Corp.). The energies of the 3D structures were minimized using semi-empirical PM3 calculations. The energy-minimized structures were then converted into .pdb files, maintaining all heavy atoms.

**LogP calculations:** cLogP values were calculated using ALOGPS 2.1 software (Virtual Computational Chemistry Laboratory) using the energy-minimized structures.<sup>[21]</sup>

**Generation of conformers:** The energy-minimized structures were combined into a single continuous pdb file for use as an input for Omega.<sup>[22]</sup> The Omega utility uses the MMFF94 force field to generate multiple conformations for each input ligand in the library in order to induce ligand flexibility in an otherwise rigid model. Modifications applied to the default settings of OMEGA were: 1) independent of conformers with an energy difference to the global minimum of > 5.0 kcal mol<sup>-1</sup> (GP\_ENERGY\_WINDOW), 2) maximum number of output conformers 400 (GP\_NUM\_OUTPUT\_CONFS), and 3) low-energy selection of conformers from the final ensemble (GP\_SELECT\_RANDOM false), with the root-mean square deviation (RMSD) cut-off of 0.8 Å (GP\_RMS\_CUTOFF). In addition, the maximum number of rotatable bonds in the molecule was raised to 30 (GP\_MAX\_ROTORS) in order to generate conformers for all ligands of our data set.<sup>[23]</sup>

**Receptor preparation:** The B-Raf V<sup>600E</sup> receptor structure was taken from the RCSB Protein Data Bank (PDB ID: 3OG7<sup>[15]</sup>) and prepared for modeling using Fast Rigid Exhaustive Docking (FRED).<sup>[24]</sup> The application allows for the creation a grid box by the mode selection pane and adjustment of its size using the mode controls. The box size should never exceed 50000–60000 Å. Once the grid box size has been adjusted, the receptor is ready for use in the docking calculations.<sup>[15]</sup>

**Docking:** Multiple scoring functions were employed in order to obtain a consensus structure and score in the final output.<sup>[25]</sup> The scoring functions include Shapegauss, Chemgauss3, Oechemscore, Screen score, and PLP. For further details of each scoring function and consensus score, see the OpenEye Scientific Software FRED manual.<sup>[24,25]</sup> Snapshots and visualization of the chemical interactions between the analogues and receptor were obtained using the VIDA application.<sup>[26]</sup>

### Chemistry

**General methods:** <sup>1</sup>H and <sup>13</sup>C NMR spectra were acquired on a Bruker AVANCE-400 MHz NMR spectrometer, in CDCl<sub>3</sub> using tetramethylsilane ( $\delta$  = 0 ppm) as the internal standard for <sup>1</sup>H NMR and the residual solvent peak ( $\delta$  = 77.16 ppm) for <sup>13</sup>C NMR. Chemical shifts ( $\delta$ ) are reported in parts per million (ppm), with coupling constants (*J*) in Hertz (Hz) and the signal multiplicities as singlet (s), doublet (d), triplet (t), quartet (q), doublet of doublets (dd), doublet of triplets (dt), multiplet (m), or broad (br). High-resolution mass spectrometry (HRMS) data were obtained using either electron ionization (EI) on a ThermoFinnigan MAT 95 XL mass spectrometer or electrospray ionization (ESI) on a ThermoFinnigan LCQ Advantage IonTrap liquid chromatography–mass spectrometer (LC/MS). Melting points (mp) were determined on a Vernier Melt Station melting point apparatus and are uncorrected. All reagents and solvents were obtained from commercial suppliers and used as received. All reactions requiring anhydrous conditions were performed in oven-dried glassware under an atmosphere of nitrogen.

**(20R,22E)-24-(*p*-fluorophenyl)-20-hydroxy-3-methoxy-19-norcho-lan-1,3,5(10),23-tetraen-22-one (MSA-3):** A stirred solution of (*i*Pr)<sub>2</sub>NH (0.57 mL, 3.70 mmol) in THF (11.6 mL) was cooled to

–78 °C, treated dropwise with *n*BuLi (2.5 M in hexanes, 1.52 mL, 3.70 mmol), and stirred at –78 °C for 1 h. A solution of  $\alpha$ -hydroxy ketone **5** (0.40 g, 1.09 mmol) in THF (2.18 mL) was then added, and the reaction was stirred for an additional 1 h at –78 °C. A solution of *para*-fluorobenzaldehyde (0.29 g, 2.18 mmol) in THF (14.5 mL) was then added at –78 °C, and the solution was allowed to slowly warm to RT and stirred for 20 h. The reaction was quenched by the addition of saturated aq NH<sub>4</sub>Cl (20 mL), followed by extraction of the aqueous layer with EtOAc (3 × 50 mL). The combined organic phases were dried over Na<sub>2</sub>SO<sub>4</sub>, filtered and concentrated in vacuo. The crude product was purified by silica gel column chromatography (hexane/EtOAc, 95:5) to yield **MSA-3** as a white solid (0.32 g, 60%); mp: 95–97 °C; <sup>1</sup>H NMR (400 MHz, CDCl<sub>3</sub>):  $\delta$  = 7.80 (d, *J* = 15.6 Hz, 1H), 7.60 (dd, *J* = 5.2, 8.8 Hz, 2H), 7.20 (d, *J* = 8.5 Hz, 1H), 7.10 (dd, *J* = 5.2, 8.8 Hz, 2H), 6.99 (d, *J* = 15.6 Hz, 1H), 6.72 (dd, *J* = 8.5, 2.7 Hz, 1H), 6.62 (d, *J* = 2.7 Hz, 1H), 4.18 (s, 1H), 3.76 (s, 3H), 2.92–2.76 (m, 2H), 2.39–2.11 (m, 3H), 1.97–1.16 (m, 11H), 1.56 (s, 3H), 0.96 ppm (s, 3H); <sup>13</sup>C NMR (100 MHz, CDCl<sub>3</sub>):  $\delta$  = 201.8, 165.5, 163.0, 157.4, 144.4, 138.0, 132.7, 130.7, 130.7, 130.6, 126.2, 118.2, 116.3, 116.1, 113.8, 111.5, 79.2, 55.7, 55.2, 55.1, 50.8, 44.3, 43.8, 43.0, 38.1, 29.8, 27.6, 26.7, 24.3, 23.7, 22.1, 13.7 ppm; HRMS (EI): *m/z* [*M*]<sup>+</sup> calcd for C<sub>30</sub>H<sub>35</sub>FO<sub>3</sub>: 462.2569, found: 462.2565.

**Methyl 2-tert-butylidimethylsilyloxy-2-methyl propanoate (2):** Methyl 2-hydroxy isobutyrate **1** (5.00 g, 42.3 mmol) was dissolved in DMF (12.5 mL), and the solution was treated with TBSCl (7.65 g, 50.75 mmol) and imidazole (7.45 g, 110.0 mmol). The reaction was allowed to stir at RT for 2 d. Saturated aq NaHCO<sub>3</sub> (30 mL) was added to the reaction, followed by the addition of hexane/EtOAc (96:4, 10 mL). The aqueous layer was extracted using hexane/EtOAc (96:4, 3 × 50 mL), and the combined organic layers were dried over Na<sub>2</sub>SO<sub>4</sub>, filtered and concentrated in vacuo. The crude material was purified using silica gel column chromatography (hexane/EtOAc, 9:1) to yield **2** as a pale yellow oil (7.00 g, 70%); <sup>1</sup>H NMR (400 MHz, CDCl<sub>3</sub>):  $\delta$  = 3.60 (s, 3H), 1.34 (s, 6H), 0.80 (s, 9H), 0.08 ppm (s, 6H); <sup>13</sup>C NMR (100 MHz, CDCl<sub>3</sub>):  $\delta$  = 175.8, 74.5, 51.4, 28.4, 25.5, 17.9, –3.2 ppm.

**2-tert-Butylidimethylsilyloxy-2-methyl propanol (3):** DIBAL-H (1.2 M in hexane, 10.0 mL, 12.0 mmol) was added to a stirred solution of ester **2** (1.27 g, 5.46 mmol) in hexane (15.6 mL) at –78 °C over 10 min, and then the solution was allowed to stir for 20 min. The reaction was warmed to RT and stirred for 20 min until TLC confirmed the disappearance of the starting material. The reaction was quenched by addition of a saturated aq solution of potassium tartrate (20 mL) at –78 °C, and the mixture was allowed to warm to RT and vigorously stirred overnight. The reaction mixture was extracted with EtOAc (3 × 50 mL), and the combined organic layers were dried over Na<sub>2</sub>SO<sub>4</sub>, filtered and concentrated in vacuo to provide **3** as colorless clear oil (1.05 g, 90%); <sup>1</sup>H NMR (400 MHz, CDCl<sub>3</sub>):  $\delta$  = 3.19 (s, 2H), 2.31 (s, 1H), 1.11 (s, 6H), 0.76 (s, 9H), 0.08 ppm (s, 6H); <sup>13</sup>C NMR (100 MHz, CDCl<sub>3</sub>):  $\delta$  = 76.3, 74.4, 28.5, 28.0, 20.3, 0.3 ppm. The crude product was used in the next reaction without further purification.

**2-tert-Butylidimethylsilyloxy-2-methyl propanal (4):** TBS-protected alcohol **3** (0.600 g, 2.93 mmol) was dissolved in CH<sub>2</sub>Cl<sub>2</sub> (29.3 mL), and 4 Å molecular sieves (0.68 g) were added. NMO (0.680 g, 5.86 mmol) was added to the stirred solution followed by the addition of TPAP (0.102 g, 0.290 mmol) at 0 °C. The reaction was allowed to stir at 0 °C for 2 h, warmed to RT, and stirred for 24 h. The reaction mixture was filtered through a pad of silica gel using Et<sub>2</sub>O as the eluting solvent. The crude product was concentrated in vacuo at low temperature using an ice bath to yield **4** as a colorless clear oil (0.300 g, 50%); <sup>1</sup>H NMR (400 MHz, CDCl<sub>3</sub>):  $\delta$  = 9.44 (s, 1H),

1.17 (s, 6H), 0.79 (s, 9H), 0.08 ppm (s, 6H); <sup>13</sup>C NMR (100 MHz, CDCl<sub>3</sub>):  $\delta$  = 206.4, 80.3, 28.0, 27.2, 20.4, 0.3 ppm. Note: The product is unstable at RT and should be stored at –20 °C; the aldehyde is stable for two weeks under argon at –20 °C.

**(20R,22E)-25-tert-butylidimethylsilyloxy-20-hydroxy-3-methoxy-19-norcholesta-1,3,5(10),23-tetraene-22-one (6):** A stirred solution of (*i*Pr)<sub>2</sub>NH (0.57 mL, 3.70 mmol) in THF (11.6 mL) was cooled to –78 °C, treated dropwise with *n*BuLi (2.5 M in hexanes, 1.52 mL, 3.70 mmol), and stirred at –78 °C for 1 h. A solution of  $\alpha$ -hydroxy ketone **5** (0.40 g, 1.09 mmol) in THF (2.18 mL) was then added, and the reaction was stirred for an additional 1 h at –78 °C. A solution of **4** (0.44 g, 2.18 mmol) in THF (14.5 mL) was added at –78 °C, and the solution was slowly warmed to RT and stirred for 20 h. The reaction was quenched by addition of saturated aq NH<sub>4</sub>Cl (20 mL), followed by extraction of the aqueous layer with EtOAc (3 × 50 mL). The combined organic phases were dried over Na<sub>2</sub>SO<sub>4</sub>, filtered, and concentrated in vacuo. The crude product was purified by silica gel column chromatography (hexane/EtOAc, 4:1) to yield **6** as an off-white solid (0.35 g, 58%); <sup>1</sup>H NMR (400 MHz, CDCl<sub>3</sub>):  $\delta$  = 7.10 (d, *J* = 8.5 Hz, 1H), 6.95 (d, *J* = 15.1 Hz), 6.60 (d, *J* = 14.9 Hz, 1H), 6.60 (dd, *J* = 8.8, 2.7 Hz, 1H), 6.51 (d, *J* = 2.52 Hz, 1H), 4.01 (s, 1H), 3.66 (s, 3H), 2.96–2.76 (m, 2H), 2.40–2.16 (m, 3H), 1.92–1.09 (m, 11H), 1.48 (s, 6H), 1.12 (s, 3H), 0.92 (s, 3H), 0.75 (s, 9H), 0.08 ppm (s, 6H); <sup>13</sup>C NMR (100 MHz, CDCl<sub>3</sub>):  $\delta$  = 204.5, 173.2, 159.4, 140.0, 134.7, 128.3, 120.3, 115.8, 113.5, 81.1, 75.6, 62.4, 57.9, 57.2, 56.9, 46.3, 45.9, 42.7, 40.2, 32.0, 29.6, 28.3, 27.9, 27.8, 27.4, 26.2, 25.7, 23.1, 20.3, 20.2, 16.2, 15.6, 0.0 ppm; HRMS (ESI): *m/z* [*M*+Na]<sup>+</sup> calcd for C<sub>33</sub>H<sub>52</sub>O<sub>4</sub>Si: 563.3535, found: 563.3527.

**(20R,22E)-20,25-dihydroxy-3-methoxy-19-norcholesta-1,3,5(10),23-tetraen-22-one (MSA-4):** TBAF (1 M in THF, 4.0 mL, 4.00 mmol) was added to a stirred solution of **6** (0.70 g, 1.29 mmol) in THF (20.0 mL), and the reaction was stirred for 6 h at RT. The reaction mixture was quenched by addition of saturated aq NH<sub>4</sub>Cl (20 mL). The aqueous layer was extracted with EtOAc (3 × 50 mL), and the combined organic layers were dried over Na<sub>2</sub>SO<sub>4</sub>, filtered and concentrated in vacuo. The crude material was purified using silica gel column chromatography (hexane/EtOAc, 4:1 → 7:3 → 3:2) to yield **MSA-4** as a white solid (0.34 g, 60%); mp: 80–83 °C; <sup>1</sup>H NMR (400 MHz, CDCl<sub>3</sub>):  $\delta$  = 7.21 (d, *J* = 8.5 Hz, 1H), 7.15 (d, *J* = 15.3 Hz, 1H), 6.71 (dd, *J* = 8.5, 2.7 Hz, 1H), 6.69 (d, *J* = 15.3 Hz, 1H), 6.63 (d, *J* = 2.8 Hz, 1H), 4.11 (s, 1H), 3.77 (s, 3H), 2.96–2.76 (m, 2H), 2.40–2.16 (m, 3H), 1.92–1.09 (m, 11H), 1.49 (s, 3H), 1.40 (s, 6H), 0.92 ppm (s, 3H); <sup>13</sup>C NMR (100 MHz, CDCl<sub>3</sub>):  $\delta$  = 202.3, 157.4, 155.9, 137.9, 132.7, 126.2, 118.1, 113.7, 111.4, 79.2, 71.3, 55.6, 55.2, 54.6, 44.3, 43.8, 40.6, 38.1, 29.8, 29.5, 27.6, 26.6, 24.1, 23.6, 21.9, 14.2, 13.6 ppm; HRMS (ESI): *m/z* [*M*+Na]<sup>+</sup> calcd for C<sub>27</sub>H<sub>38</sub>O<sub>4</sub>: 449.2669, found: 449.2662.

**(20R)-3-Methoxy-20-hydroxy-19,24-dinorcholan-1,3,5(10),9(11)-tetraen-22-one (7):** A solution of DDQ (0.41 g, 1.80 mmol) in MeOH (15.0 mL) was added to a stirred solution of **5** (0.50 g, 1.40 mmol) in CH<sub>2</sub>Cl<sub>2</sub> (7.0 mL) via syringe at 0 °C, and the reaction was allowed to warm to RT. The color of the reaction mixture turned brown upon addition of DDQ and then faded over time. The reaction was stirred for 1 h until TLC confirmed the disappearance of all starting material. The reaction mixture was concentrated in vacuo, and the crude material was purified using silica gel column chromatography (hexane/EtOAc, 9:1) to yield **7** as a white solid (0.40 g, 80%); mp: 125–128 °C; <sup>1</sup>H NMR (400 MHz, CDCl<sub>3</sub>):  $\delta$  = 7.53 (d, *J* = 8.8 Hz, 1H), 6.72 (dd, *J* = 8.8, 2.7 Hz, 1H), 6.59 (d, *J* = 2.8 Hz, 1H), 6.09 (m, 1H), 4.00 (s, 1H), 3.79 (s, 3H), 2.95–2.75 (m, 2H), 2.36–2.11 (m, 2H), 2.23 (s, 2H), 1.94–1.15 (m, 10H), 1.48 (s, 3H), 0.94 ppm (s, 3H); <sup>13</sup>C NMR (100 MHz, CDCl<sub>3</sub>):  $\delta$  = 211.8, 158.3,

137.5, 134.9, 127.3, 125.1, 117.5, 113.2, 112.6, 80.0, 55.2, 52.7, 43.1, 42.3, 38.1, 30.0, 28.6, 24.7, 24.3, 23.3, 22.2, 13.6 ppm; HRMS (EI):  $m/z$   $[M]^+$  calcd for  $C_{23}H_{30}O_3$ : 354.2189, found: 354.2196. Note: the  $R_f$  values of the product and starting material are so close that they require multiple runs on the TLC plate using hexane/EtOAc (9:1) for separation.

**(20R,22E)-25-tert-Butyldimethylsilyloxy-20-hydroxy-3-methoxy-19-norcholesta-1,3,5(10),9(11),23-pentaen-22-one (8):** A stirred solution of  $(iPr)_2NH$  (0.57 mL, 3.70 mmol) in THF (11.6 mL) was cooled to  $-78^\circ C$ , treated dropwise with  $nBuLi$  (2.5 M in hexanes, 1.52 mL, 3.70 mmol), and stirred at  $-78^\circ C$  for 1 h. A solution of **7** (0.40 g, 1.09 mmol) in THF (2.18 mL) was then added, and the reaction was stirred for an additional 1 h at  $-78^\circ C$ . A solution of **4** (0.44 g, 2.18 mmol) in THF (14.5 mL) was then added at  $-78^\circ C$ , and the solution was slowly warmed to RT and stirred for 20 h. The reaction was quenched by the addition of saturated aq  $NH_4Cl$  (20 mL), followed by extraction of the aqueous layer with EtOAc (3  $\times$  50 mL). The combined organic layers were dried over  $Na_2SO_4$ , filtered and concentrated in vacuo. The crude product was purified by silica gel column chromatography (hexane/EtOAc, 4:1) to yield **8** as a white solid (0.36 g, 60%);  $^1H$  NMR (400 MHz,  $CDCl_3$ ):  $\delta$  = 7.42 (d,  $J$  = 8.8 Hz, 1H), 6.97 (d,  $J$  = 14.9 Hz, 1H), 6.61 (d,  $J$  = 14.9 Hz, 1H), 6.60 (dd,  $J$  = 8.8, 2.7 Hz, 1H), 6.48 (d,  $J$  = 2.5 Hz, 1H), 5.99 (m, 1H), 4.06 (s, 1H), 3.67 (s, 3H), 2.83–2.65 (m, 2H), 2.47–2.14 (m, 2H), 1.92–1.09 (m, 10H), 1.48, (s, 6H), 1.12 (s, 2H), 0.92 (s, 3H), 0.81 (s, 9H), 0.08 ppm (s, 6H);  $^{13}C$  NMR (100 MHz,  $CDCl_3$ ):  $\delta$  = 204.5, 160.4, 159.4, 139.6, 136.9, 129.4, 127.4, 120.2, 119.7, 115.3, 114.7, 81.0, 75.6, 57.3, 57.0, 54.8, 45.1, 44.3, 40.2, 32.3, 32.1, 31.9, 30.6, 27.9, 26.8, 25.9, 24.1, 20.3, 15.7, 0.0 ppm; HRMS (ESI):  $m/z$   $[M+Na]^+$  calcd for  $C_{33}H_{50}O_4Si$ : 561.3371, found: 561.3376.

**(20R,22E)-20,25-Dihydroxy-3-methoxy-19-norcholesta-1,3,5(10),9(11),23-pentaen-22-one (MSA-5):** TBAF (1 M in THF, 4.0 mL, 4.00 mmol) was added to a stirred solution of **8** (0.70 g, 1.29 mmol) in THF (20.0 mL), and the reaction was stirred for 6 h at RT. The reaction mixture was quenched by addition of a saturated aq  $NH_4Cl$  (20 mL). The aqueous layer was extracted with EtOAc (3  $\times$  50 mL), and the combined organic layers were dried over  $Na_2SO_4$ , filtered and concentrated in vacuo. The crude material was purified using silica gel column chromatography (hexane/EtOAc, 4:1  $\rightarrow$  7:3  $\rightarrow$  3:2) to yield **MSA-5** as a white solid (0.38 g, 70%); mp: 88–90;  $^1H$  NMR (400 MHz,  $CDCl_3$ ):  $\delta$  = 7.52 (d,  $J$  = 9.1 Hz, 1H), 7.15 (d,  $J$  = 15.1 Hz, 1H), 6.71 (dd,  $J$  = 8.8, 2.7 Hz, 1H), 6.68 (d,  $J$  = 15.3 Hz, 1H), 6.59 (d,  $J$  = 2.5 Hz, 1H), 6.08 (m, 1H), 4.15 (s, 1H), 3.78 (s, 3H), 2.96–2.76 (m, 2H), 2.40–2.16 (m, 2H), 1.92–1.09 (m, 10H), 1.50 (s, 3H), 1.39 (s, 6H), 0.95 ppm (s, 3H);  $^{13}C$  NMR (100 MHz,  $CDCl_3$ ):  $\delta$  = 202.4, 158.3, 156.2, 137.5, 134.8, 127.4, 125.1, 118.0, 117.6, 113.3, 112.6, 79.1, 71.2, 55.2, 54.7, 52.6, 42.9, 42.3, 38.1, 30.1, 29.5, 29.4, 28.6, 24.7, 23.8, 22.1, 13.8 ppm; HRMS (EI):  $m/z$   $[M]^+$  calcd for  $C_{27}H_{36}O_4$ : 424.2614, found: 424.2608.

### Biological screening

**MTT assay:** **MSA-1**, **MSA-2**, and **MSA-3** were dissolved in 1% DMSO and 0.01% Tween 80; **MSA-4** and **MSA-5** were dissolved in 1% DMSO alone. A-375 cells were seeded in 96-well plates at 30000 cells per well and incubated for 24 h at  $37^\circ C$  and 5%  $CO_2$ . The cells were treated with test compound (fivefold serial dilution) for 48 h at  $37^\circ C$  and 5%  $CO_2$  in the incubator. Finally, the cells were treated with 5.0  $mg\ mL^{-1}$  3-(4,5-dimethylthiazol-2-yl)-2,5-diphenyltetrazolium bromide (MTT) in phosphate-buffered saline (PBS), purchased from Sigma-Aldrich, for 4 h and lysed with 0.01 N HCl containing 10% sodium dodecyl sulfate (SDS). Plates were read on

a Biotech plate reader at 570 nm 4 h after lysing. The  $IC_{50}$  value was determined from the exponential curve of viability versus concentration. The viability was calculated using Equation (1), where  $A_{drug}$  is the absorbance at 570 nm for the compound,  $A_{NC}$  is the absorbance for the negative control (no cells), and  $A_{PC}$  is the absorbance of positive control (cells with no drug). The experiments were run at least in triplicates, along with negative and positive controls.

$$\text{Viability (\%)} = 100 \cdot \frac{(A_{drug} - A_{NC})}{(A_{PC} - A_{NC})} \quad (1)$$

**Enzyme-linked immunosorbent assay (ELISA):** Thermo Scientific Pierce ERK1/2 colorimetric in-cell ELISA kit, including buffers, target-specific primary antibodies (anti-ERK1/2 (Thr202/Tyr204) and anti-ERK1/2 antibodies), and horseradish peroxidase (HRP)-conjugated detection reagent, was used. A-375 cells were seeded in 96-well plates at 20000 cells per well in the corresponding medium, and incubated at  $37^\circ C$  for 24 h. Cells were treated with test compounds and PLX-4032 for different time intervals, then stimulated with EGF (100  $ng\ mL^{-1}$ ) prior to fixation using 4% formaldehyde. Permeabilization buffer, quenching solution, and blocking buffer were added to the fixed cells, which were then treated with primary antibody and incubated overnight. Then, HRP conjugate was added followed by 3,3',5,5'-tetramethylbenzidine (TMB) substrate and TMB stop solution. The absorbance was measured using an ELISA plate reader at 450 nm, and the collected data was normalized by staining the whole cell using Janus green, followed by measuring absorbance again at 615 nm. The experiments were run at least in triplicate.

### Acknowledgements

The authors would like to acknowledge South Dakota Board of Regents-2010 Biological Control and Analysis by Applied Photonics (BCAAP) Center for financial support, OpenEye Scientific Software Inc. (Santa Fe, USA) for providing an academic license for the molecular modeling software, and Dr. Alice Bergmann (University of Buffalo, USA) for performing high-resolution mass spectrometry; the mass spectrometers used by Dr. Bergmann were obtained through the Chemistry Research Instrumentation and Facilities (CRIF) Program of the National Science Foundation (award CHE0091977).

**Keywords:** anticancer agents • B-Raf • cucurbitacins • kinases • molecular modeling • natural products

- [1] a) M. Lahlou, *Pharmacol. Pharm.* **2013**, *4*, 17–31; b) D. Dias, S. Urban, U. Roessner, *Metabolites* **2012**, *2*, 303–336; c) B. Mishra, V. Tiwari, *Eur. J. Med. Chem.* **2011**, *46*, 4769–4807; d) D. Newman, G. Cragg, *J. Nat. Prod.* **2012**, *75*, 311–335.
- [2] a) A. Alghasham, *Int. J. Health Sci.* **2013**, *7*, 77–89; b) X. Chen, J. Bao, J. Guo, Q. Ding, J. Lu, M. Huang, Y. Wang, *Anti-Cancer Drugs* **2012**, *23*, 777–787; c) D. Lee, G. Iwanski, N. Thoenissen, *Sci. World J.* **2010**, *10*, 413–418; d) J. Chen, M. Chiu, R. Nie, G. Cordell, S. Qiu, *Nat. Prod. Rep.* **2005**, *22*, 386–399.
- [3] a) W. Chen, W. Tang, L. Lou, W. Zhao, *Phytochemistry* **2006**, *67*, 1041–1047; b) R. Fuller, J. Cardellina II, G. Cragg, M. Boyd, *J. Nat. Prod.* **1994**, *57*, 1442–1445; c) J. Li, Y. Zhang, D. Ouyang, L. Xu, H. Mo, X. He, *Afr. J. Pharm. Pharmacol.* **2012**, *6*, 1545–1554; d) J. M. Siqueira, A. C. Gazola, M. R. Farias, L. Volkov, N. Rivard, A. J. Brum-Fernandes, R. M. Ribeiro-do-Valle, *Cancer Chemother. Pharmacol.* **2009**, *64*, 529–538; e) H. Oh, Y. Mun, S. Im, H. Song, H. Lee, W. Woo, *Planta Med.* **2002**, *68*, 832–833.

- [4] a) M. S. Ahmed, F. Halaweish, *J. Enzyme Inhib. Med. Chem.* **2014**, *29*, 162–167; b) K. Chan, F. Meng, Q. Li, C. Ho, T. Lam, Y. To, W. Lee, M. Li, K. Chu, M. Toh, *Cancer Lett.* **2010**, *294*, 118–124; c) K. Chan, K. Li, S. Liu, K. Chu, M. Toh, W. Xie, *Cancer Lett.* **2010**, *289*, 46–52.
- [5] H. Davies, G. Bignell, C. Cox, P. Stephens, S. Edkins, S. Clegg, J. Teague, H. Woffendin, M. Garnett, W. Bottomley, N. Davis, E. Dicks, R. Ewing, Y. Floyd, K. Gray, S. Hall, R. Hawes, J. Hughes, V. Kosmidou, A. Menzies, C. Mould, A. Parker, C. Stevens, S. Watt, S. Hooper, R. Wilson, H. Jayatilake, B. Gusterson, C. Cooper, J. Shipley, D. Hargrave, K. Pritchard-Jones, N. Maitland, G. Chenevix-Trench, G. Riggins, D. Bigner, G. Palmieri, A. Cossu, A. Flanagan, A. Nicholson, J. Ho, S. Leung, S. Yuen, B. Weber, H. Seigler, T. Darrow, H. Paterson, R. Marais, C. Marshall, R. Wooster, M. Stratton, P. Futreal, *Nature* **2002**, *417*, 949–954.
- [6] a) P. Pollock, P. Meltzer, *Cancer Cell* **2002**, *2*, 5–7; b) P. Ascierto, J. Kirkwood, J. Grob, E. Simeone, A. Grimaldi, M. Maio, G. Palmieri, A. Testori, F. Marincola, N. Mozzillo, *J. Transl. Med.* **2012**, *10*, 85.
- [7] a) M. Gabrielsen, M. Schldt, J. Munro, D. Borucka, J. Cameron, M. Baugh, A. Mleczak, S. Lilla, N. Morrice, M. F. Olson, *Cell Commun. Signaling* **2013**, *11*, 58; b) Indian Council of Medical Research Task Force (ICMRTF) New Delhi, India, *Indian J. Med. Res.* **2012**, *135*, 49–55; c) R. Puri, R. Sud, A. Khaliq, M. Kumar, S. Jain, *Indian J. Gastroenterol.* **2011**, *30*, 233–236.
- [8] a) O. K. Radjasa, Y. M. Vaske, G. Navarro, H. C. Vervoort, K. Tenney, R. G. Linington, P. Crews, *Bioorg. Med. Chem.* **2011**, *19*, 6658–6674; b) B. K. S. Yeung, *Curr. Opin. Chem. Biol.* **2011**, *15*, 523–528; c) C. R. Strader, C. J. Pearce, N. H. Oberlies, *J. Nat. Prod.* **2011**, *74*, 900–907; d) F. Feyen, F. Ca-choux, J. Gertsch, M. Wartmann, K. Altmann, *Acc. Chem. Res.* **2008**, *41*, 21–31.
- [9] a) R. H. Guo, C. A. Geng, X. Y. Huang, Y. B. Ma, Q. Zhang, L. J. Wang, X. M. Zhang, R. P. Zhang, J. J. Chen, *Bioorg. Med. Chem.* **2013**, *23*, 1201–1205; b) K. L. Lang, I. T. Silva, L. A. Zimmermann, V. R. Machado, M. R. Teixeira, M. I. Lapuh, M. A. Galetti, J. A. Palermão, G. M. Cabrera, L. S. C. Bernardes, C. M. O. Simões, E. P. Schenkel, M. S. B. Caro, F. J. Durán, *Bioorg. Med. Chem.* **2012**, *20*, 3016–3030; c) J. Bartalis, F. T. Halaweish, *Bioorg. Med. Chem.* **2011**, *19*, 2757–2766.
- [10] a) H. Matsuda, S. Nakashima, O. Abdel-Halim, T. Morikawa, M. Yoshikawa, *Chem. Pharm. Bull.* **2010**, *58*, 747–751; b) C. Chen, S. Qiang, L. Lou, W. Zhao, *J. Nat. Prod.* **2009**, *72*, 824–829; c) X. Fang, C. H. Phoebe, Jr., J. M. Pezzuto, H. H. S. Fong, N. R. Farnsworth, *J. Nat. Prod.* **1984**, *47*, 988–993.
- [11] a) S. L. Acebedo, F. Alonso, J. A. Ramírez, L. R. Galagovsky, *Tetrahedron* **2012**, *68*, 3685–3691; b) S. Parihar, A. Gupta, A. K. Chaturvedi, J. Agarwal, S. Luqman, B. Changkija, M. Manohar, D. Chanda, C. S. Chanotiya, K. Shanker, A. Dwivedi, R. Konwar, A. S. Negi, *Steroids* **2012**, *77*, 878–886; c) S. Farhane, M. Fournier, R. Maltais, D. Poirier, *Tetrahedron* **2011**, *67*, 2434–2440; d) Y. Matsuya, S. Masuda, N. Ohsawa, S. Adam, T. Tschamber, J. Eustache, K. Kamoshita, Y. Sukenaga, H. Nemoto, *Eur. J. Org. Chem.* **2005**, 803–808; e) L. F. Tietze, G. Schneider, J. Wölfling, A. Fecher, T. Nöbel, S. Petersen, I. Schuberth, C. Wulff, *Chem. Eur. J.* **2000**, *6*, 3755–3760.
- [12] a) S. Sinha, S. Roy, B. S. Reddy, K. Pal, G. Sudhakar, S. Iyer, S. Dutta, E. Wang, P. K. Vohra, K. R. Roy, P. Reddanna, D. Mukhopadhyay, R. Banerjee, *Mol. Cancer Res.* **2011**, *9*, 364–374; b) A. O. Mueck, H. Seeger, *Steroids* **2010**, *75*, 625–631; c) P. Bunyathaworn, S. Boonananwong, B. Kongkathip, N. Kongkathip, *Steroids* **2010**, *75*, 432–444; d) J. W. Simpkins, S. H. Yang, R. Liu, E. Perez, Z. Y. Cai, D. F. Covey, P. S. Green, *Stroke* **2004**, *35*, 2648–2651.
- [13] a) R. T. Kroemer, *Curr. Protein Pept. Sci.* **2007**, *8*, 312–328; b) X. Kong, J. Qin, Z. Li, A. Vultur, L. Tong, E. Feng, G. Rajan, S. Liu, J. Lu, Z. Liang, M. Zheng, W. Zhu, H. Jiang, M. Herlyn, H. Liu, R. Marmorstein, C. Luo, *Org. Biomol. Chem.* **2012**, *10*, 7402–7417; c) H. Park, H. Choi, S. Hong, S. Hong, *Bioorg. Med. Chem. Lett.* **2011**, *21*, 5753–5756; d) C. Luo, P. Xie, R. Marmorstein, *J. Med. Chem.* **2008**, *51*, 6121–6127.
- [14] a) P. C. D. Hawkins, A. Nicholls, *J. Chem. Inf. Model.* **2012**, *52*, 2919–2936; b) P. C. D. Hawkins, A. G. Skillman, G. L. Warren, B. A. Ellingson, M. T. Stahl, *J. Chem. Inf. Model.* **2010**, *50*, 572–584.
- [15] M. McGann, *J. Chem. Inf. Model.* **2011**, *51*, 578–596.
- [16] L. C. Kopel, M. S. Ahmed, F. T. Halaweish, *Steroids* **2013**, *78*, 1119–1125.
- [17] K. Denmark, R. Stavenger, *J. Am. Chem. Soc.* **2000**, *122*, 8837–8847.
- [18] E. J. Corey, A. Venkateswarlu, *J. Am. Chem. Soc.* **1972**, *94*, 6190–6191.
- [19] J. Doussot, R. Garreau, L. Dallery, P. Guette, A. Guy, *Bull. Soc. Chim. Fr.* **1995**, *132*, 59–66.
- [20] M. Otagiri, *Drug Metab. Pharmacokinet.* **2005**, *20*, 309–323.
- [21] I. V. Tetko, P. Bruneau, *J. Pharm. Sci.* **2004**, *93*, 3103–3110.
- [22] OMEGA, version 2.2.1; OpenEye Scientific Software, Santa Fe, NM (USA). <http://www.eyesopen.com>.
- [23] E. Kellenberger, J. Rodrigo, P. Muller, D. Rognan, *Proteins Struct. Funct. Bioinf.* **2004**, *57*, 225–242.
- [24] Fast Rigid Exhaustive Docking (FRED) Receptor, version 2.2.5; OpenEye Scientific Software, Santa Fe, NM (USA); <http://www.eyesopen.com>.
- [25] Fast Rigid Exhaustive Docking (FRED), version 2.2.3; OpenEye Scientific Software, Santa Fe, NM (USA). <http://www.eyesopen.com>.
- [26] VIDA, version 4.1.2; OpenEye Scientific Software, Santa Fe, NM (USA). <http://www.eyesopen.com>.

Received: December 12, 2013

Published online on March 28, 2014